Effect of X-ray Irradiation on Electrical Characteristics Of Au/n-Bi_2Te_3/p-Si/Al diodes.

Ahmed A. Khodiri, Ahmed M. Nawar, and K.M Abd El-kader

Department of Physics, Faculty of Science, Suez Canal University,

Abstract

The Au/n-Bi_2Te_3/psi/Al diode has been fabricated by using a thermal evaporation technique. The fabricated diodes were divided into two groups, the first group was as-fabricated diode, and the second group was irradiated by 6 MeV X-ray. The two groups were characterized by temperature dependent current-voltage (I-V) measurements in the range from 308 K to 373 K. The conduction mechanisms governed by the thermionic emission (TE) at lower forward voltages and the space charge-limited current (SCLC) dominated by single trap level at higher forward voltages. The junction parameters are estimated as a function of temperature. The junctions are non-ideal in showing ideality factor of 2.67 and 3.03 for as-fabricated and irradiated junctions at 308 K, respectively. The series resistances, rectification ratio and potential barrier height were also investigated.

1. Introduction

Semiconducting Chalcogenide thin films have received enormous attention in the recent years because of a broad range of their applications in the various fields of science and technology. Among the various V-VI compounds, Bismuth Telluride (Bi_2Te_3) is a power generator and sensors or detectors [1,2]. The studies of the electronic properties of semiconductors have been mainly stimulated by gorgeous micro-electronic device applications. Semiconductor devices are the most sensitive to the radiation induced damages produced by energetic γ-rays, electrons, neutrons and ions. An exposure of these devices to such radiations results in the creation of considerable quantity of lattice defects [3–6].

The nature of forming defects depends on the form of radiation. While irradiation with the X-ray, γ-rays and electrons produces mainly isolated point defects, irradiation with heavier ions produces more complex cluster of defects [6-9].The analysis of current – voltage (I-V) characterization of the Schottky diodes only at room temperature does not give full data about their current transport mechanisms or the nature of barrier establishment. Nevertheless, the current – voltage (I-V) characterization allows us to understand the different characteristics of the device. In general, the forward bias characteristics of these devices in general deviate from the ideal thermionic emission (TE) theory [10-15].

In this work, we explore the high energy X -ray irradiation effects on the electric and dielectric properties of an Au/Bi_2Te_3/p-Si/Al Schottky barrier diode exposed to a dose of 10 Gy. Diode characteristics, pre and post- irradiation, were investigated using I–V measurements in the temperature range of 308-373 K.

2. Experimental Part

2.1 Device construction

The p-Si wafer was etched in a solution containing hydro-fluoric, nitric and acetic acids in the ratio of 1:6:1 to eliminate the native oxide. After etching process, the p-Si wafer was immersed and washed with distilled water then with ethyl alcohol. The p-Si wafer was inserted in a vacuum coating unit, and the back side electrode of Si wafer was made by coating it with a thick pure aluminum film. On the front side of the p-Si wafer substrate, a thin layer (55 nm) of Bi_2Te_3 was deposited through a special mask followed by deposition of thin film of pure gold through another one Fig.1 represent a Schematic diagram of the Au/n-Bi_2Te_3/p-Si/Al diode diode. The device was constructed with an active area of 6.3×10^{-3} cm^2.

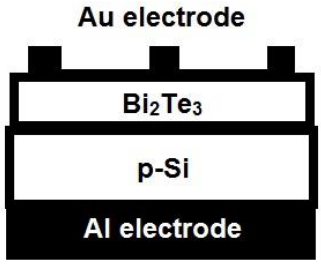

Figure 1. Schematic diagram of the Au/n-Bi_2Te_3/p-Si/Al diode diode

The thin films of Bi_2Te_3 in this study were thermally deposited on the substrates by using a high-vacuum coating unit (model E306 A, Edwards Co.-England); the pressure inside the coating chamber was pumped down to 4×10^{-4} Pa before starting the evaporation process. The gold and aluminum electrodes were evaporated directly from the basket-shaped tungsten filament and Horizontal Helix filament, respectively.

2.2 The High-Current Linear Accelerator Unit

The diode was irradiated with 6 MeV X-rays generated from the linear electron accelerator [16]. The output X-ray radiation beam calibrated using (UNIDOS E T10008-80685 Electrometer, TM30010-03870 Ionization Chamber, PTW Freiburg, Germany).

2.3 Measurements

An X-ray diffractometer (Philips X00 pert, Pro.) with filtered CuKα radiation was used to investigate the structural properties of the Bi_2Te_3 in powder and thin-film forms for the (2θ) diffraction angle range

(10-60°). For the measurements of current versus voltage (I-V) at different temperatures for the devices, stabilized power supply and high impedance electrometer (Keithly 617) was used.

3. Results and discussion

3.1 X-ray diffraction analysis

Figure 2 shows the spectrum of X-ray powder diffraction for Bi_2Te_3 in powder form was taken in a 2θ range from 10° to 60°.

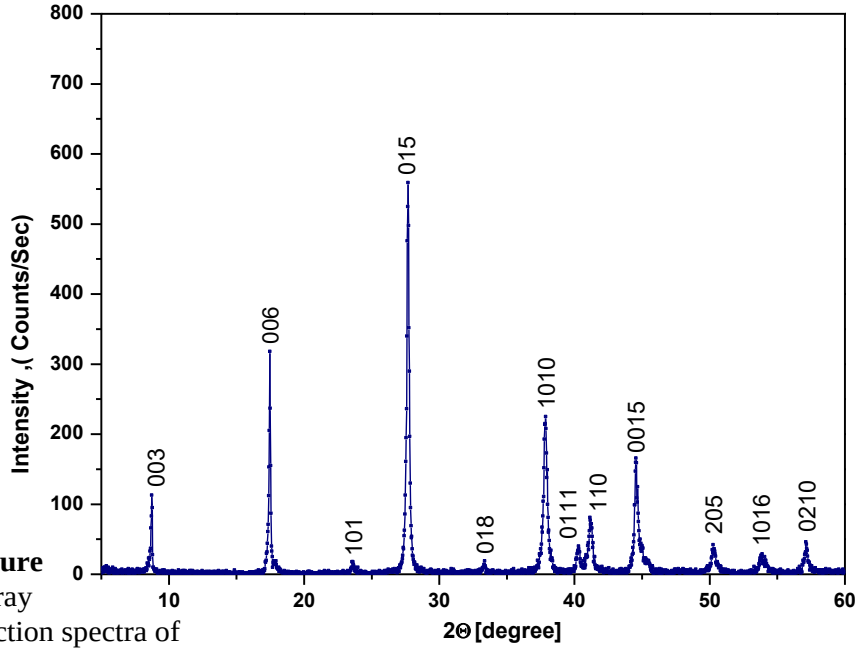

Figure 2 X-ray diffraction spectra of Bi_2Te_3 powder

The pattern has many diffraction peaks with different intensities which specifying that the powder of Bi_2Te_3 has a polycrystalline nature. The maximum intensity is found with the (015) plane. The unit cell parameters of Bi_2Te_3 in powder form were determined, and the parameters found to be a = 4.381 Å and c =30.437 Å. All the diffraction peaks in the patterns of all the powder products correspond to the peaks of rhombohedral Bi_2Te_3 (ICDD no. 15-0863) with space group: R3m (166).

Table 1 displays the values of Miller indices, (h k l), for the maximum values of diffraction peak together with the interplanar spacing, (d_{hkl}), and our check cell is in agreement with [17-21].

Table 1. The diffraction spacing, d measured, the Miller indices (h k l), and the relative intensity, I/I_o, for Bi_2Te_3 in the powder form.

Peak No.	**2θ (degree) measured**	**d(A°) measured**	**d(A°) calculated**	**I/I_o**	**hkl**
1	17.46732	5.07292	5.07305	57.60	006
2	27.68051	3.22002	3.22010	100.00	015
3	37.84259	2.37543	2.37549	38.76	$10\bar{1}0$
4	41.14973	2.19184	2.19189	14.38	110
5	44.54489	2.03234	2.03239	29.19	$0015\bar{}$

3.2 Dark current – voltage characteristics

The dark direct current (DC) characteristics of Au/Bi_2Te_3/p-Si/Al diode Schottky diode are measured at different temperatures ranging from 308 to 373 K and in the voltage range from -2 to 2 V, the diode behavior of the two junctions groups; pre-irradiation and post-irradiation is shown in **Figure 3.a and 3.b.**

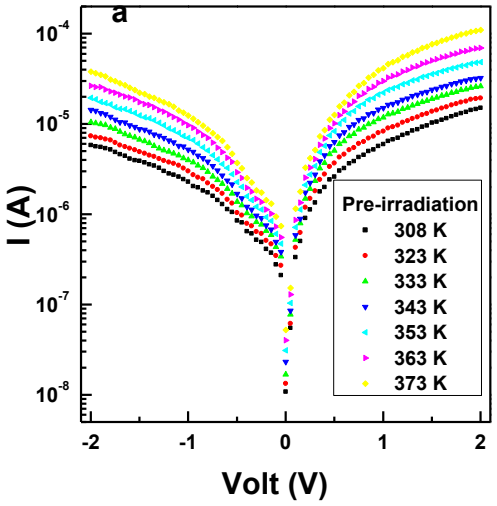

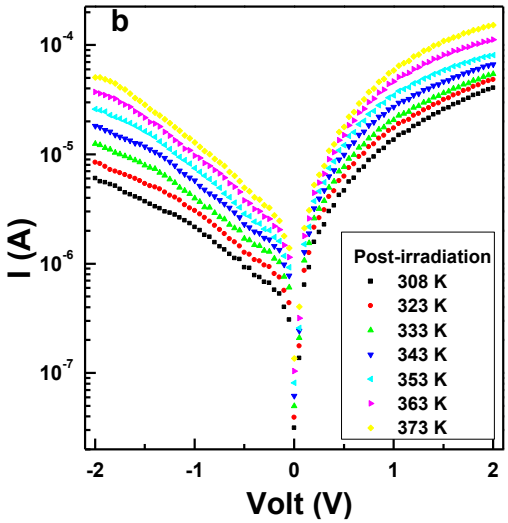

Figure 3. I–V–T characteristics of (a) pre-irradiated Au/n-Bi_2Te_3/psi/Al junction (b) post-irradiated Au/n-Bi_2Te_3/p-Si/Al junction.

The results characterize a behavior of typical diode and at a certain applied voltage the current increases with increasing temperature, indicating a negative temperature coefficient for the resistivity [22-23].

The discontinuity appears at V = 0 may because of the formation of the electrical double layer on the surface of the electrode. Also, the results show an existence of leakage current in the reverse bias direction.

The rectification ratio (RR) estimated to be 2.60 at ± 1V at temperature 308 K and increase to be 6.25 with X-ray irradiation process. **Table 2** shows that the rectification ratio decreases with increasing temperature; this is due to the increase in leakage current with increasing temperature [23].

The natural logarithmic plot of forward current characteristics versus voltage at fixed temperature 308 K pre-irradiation and the post-irradiation process of Au/Bi_2Te_3/p-Si/Al device are shown in **Figure 4**.

At applied potentials less than 0.5 V, the logarithm of the current increases linearly with increasing applied voltage; this indicates that thermionic emission conduction is the predominant conduction mechanism in such a potential range. [24].

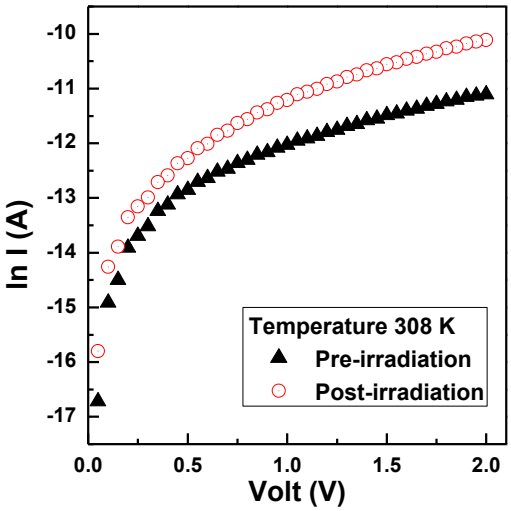

Figure 4. Dark forward bias I-V characteristics of Au/Bi_2Te_3/p-Si/Al diode diode are measured at 308 K.

The current to the applied bias in this region by:

$$I = I_S \exp\left(\frac{q(V-IR_s)}{nTK_B} - 1\right)\left[1 - \exp\left(\frac{-q(V-IR_s)}{TK_B}\right)\right] \quad (1)$$

Where q is the electron charge, and refers to the ideality factor, k_B is the Boltzmann constant, T is the absolute temperature, V is the applied potential, the term IR_S represents the potential drop across the series resistance R_S and I_S refers the reverse saturation current, which is given by:

$$I_s = AA^*T^2 \exp\left(\frac{-q\emptyset_{bi}}{TK_B}\right) \quad (2)$$

A is the diode area (6.3×10^{-3} cm^2), A* is the effective Richardson constant (32 A cm^{-2} K^2 for p-type Si [24-26]), Φ_{bi} is the zero-bias barrier height. The saturation current was acquired at different temperatures from the intercept of the linear part in a semi-logarithmic plot versus the current axis at zero voltage **Figure 5**. The diode ideality factor n and the built- in potential Φ_{bi} can be deduced from early Equations as:

$$n = \frac{e}{TK_B}\frac{d(V-IR_s)}{d\ln(I)} \quad (3)$$

and

$$\emptyset_{bi} = \frac{TK_B}{e}\ln\frac{AA^*T^2}{I_s} \quad (4)$$

The values of the ideality factor were estimated from the of the acquired straight lines at low voltage region **Figure 4**, the junction performance was non-ideal due to the ideality factor values was more than unity. The ideality factor value is probably affected by a result of electrons and hole recombination in the

depletion region and/or the increase of diffusion current due to the applied voltage value was increased [27].

The value of barrier height obtained from the current-voltage characteristics using Eq.4. is found to be 0.65 eV and 0.62 eV for pre-irradiation and post-irradiation, respectively. The change of n and Φ_{bi} with temperature for pre-irradiation and the post-irradiation process was tabulated in **Table 2**.

The series resistance, R_s, is an important parameter, however, it affects the electrical characterization of the rectifying contacts. R_s in diode junction occur as a result of the contact resistance between metal-semiconductor interface, Ohmic resistance in metal contacts and Ohmic resistance of the semiconductor material. A semi-logarithmic plot of the forward current versus an applied voltage at 308 K for a temperature simple explanation is shown in **Figure 5**. Thus, the voltage drop, $\Delta V = IR_s$, across the unbiased region for a given forward current, I, given by the horizontal displacement between the actual arc and the extrapolated linear part given [28].

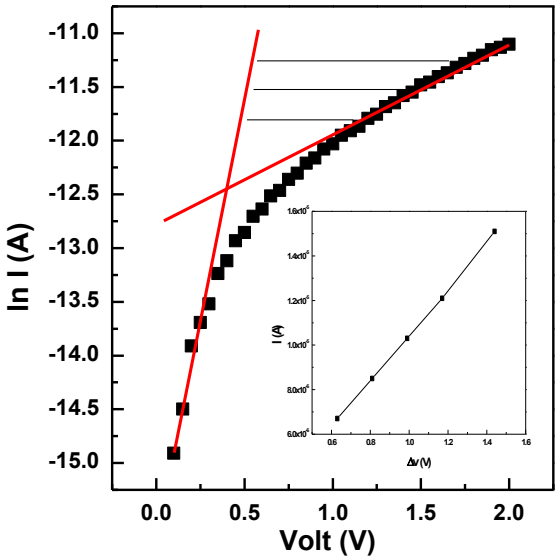

Figure 5. The junction I-V characteristics of Au/Bi_2Te_3/p-Si/Al diode at 308 K. Inset is the voltage drop across the series resistance.

The plot of ΔV versus I, as shown in the inset of **Figure 5**, gives a straight line, the slope provides the value of the series resistance, = 97.09, 29.76 KΩ for pre-irradiation and post-irradiation, respectively. The values of R_s in the temperature range (308K-373K) for pre-irradiation and the post-irradiation process were tabulated in **Table 2**.

The series resistance is calculated according to Lien, So, and Nicolet method [29], this method used to determine the series resistance, especially for the high series resistance values, this method is based upon an auxiliary function:

$$G_\gamma(V,I) = \frac{V}{\gamma} - \frac{KT}{q}\ln\left(\frac{I}{AA^*T^2}\right) \quad (5)$$

Where γ is an arbitrary parameter greater than n. Plots of G_γ(V,I) vs I show a minimum for $I_{o\gamma}$=(kT/qRs)(γ-n). The plot of $I_{o\gamma}$ vs γ is a straight line whose slope leads to the value of the series resistance Rs the values of series resistance listed in **Table 2**. From the value of G_γ(V,I) and the corresponding current I_o at the minimum, the barrier height value can be obtained:

$$\emptyset_{bi} = G(V,I) + \frac{V}{\gamma} - \frac{KT}{q} \quad (6)$$

Table 2. Typical parameters obtained from (I-V) measurements.

T (K)	RR		n		R_s (KΩ)		R_s (KΩ) (Lien)		Φ_b(eV)		Φ_b(eV) (Lien)	
	Pre	Post	pre	post	Pre	post	Pre	post	pre	Post	pre	Post
308	2.61	6.25	2.67	3.03	97.09	29.76	155.77	62.16	0.65	0.62	0.66	0.63
323	2.76	5.67	2.42	2.85	78.93	26.67	107.22	96.92	0.68	0.65	0.68	0.65
333	2.95	5.20	2.33	2.75	62.66	25.97	50.99	44.52	0.70	0.67	0.72	0.68
343	2.89	5.70	2.22	2.60	53.25	22.32	65.78	27.64	0.72	0.68	0.73	0.69
353	3.16	4.63	2.15	2.46	38.91	20.16	30.14	21.06	0.73	0.70	0.75	0.71
363	3.11	4.78	2.11	2.42	23.31	14.45	20.68	15.26	0.75	0.72	0.78	0.74
373	3.35	4.55	2.03	2.40	13.22	9.71	21.84	8.32	0.76	0.73	0.78	0.76

From **Table 2**, it can be seen that there is a good agreement between the values of the barrier height deduced by thermionic emission theory and those obtained from Lien, So, and Nicolet method. If, on the other hand, the value of the series resistance obtained from Lien, So, and Nicolet function is larger than the values obtained from (I-ΔV) curve and that because of (I-ΔV) method applied to the high voltage region for the forward bias. Beside, Lien, So, and Nicolet function applied to the full forward bias of the diode junction.

The obtained values of ideality factor and barrier height are plotted against temperature as shown in **Figure 6.a and 6.b**. It is seen that with increasing temperature, the value of barrier height increases while ideality factor decreases. This high value of ideality factor (that is, n > 2) suggests that the I-V characteristic of the studied diode was not limited by the forward biased current behavior of the conventional p-n junction. The deviation of n from unity shows that the device is not ideal. [30]. Defects at the interface may play important

roles in the conduction process of the diode [31-35].

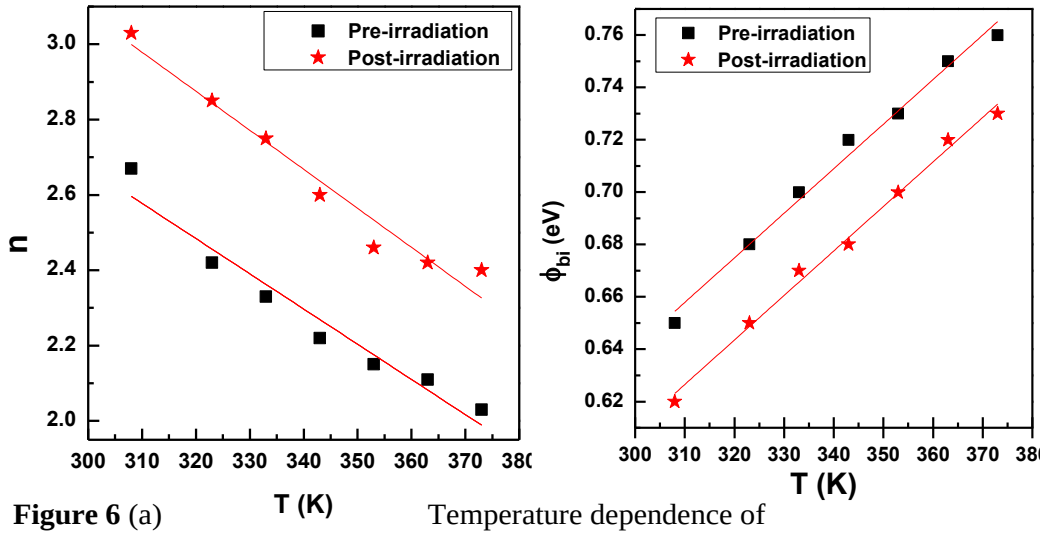

Figure 6 (a) Temperature dependence of ideality factor (n), and (b) Temperature dependence of barrier height (Φ) of $Au/Bi_2Te_3/p\text{-}Si/Al$ diode.

The value of barrier height decreases while ideality factor increases after irradiation process. At relatively higher voltages > 0.5, the current density shows a power law dependence of the form $J_F \alpha V^m$ where m~2 is shown in **Figure 7.a and 7.b**. indicating that the dark current is governed by space charge-limited current (SCLC) dominated by single trap level [36].

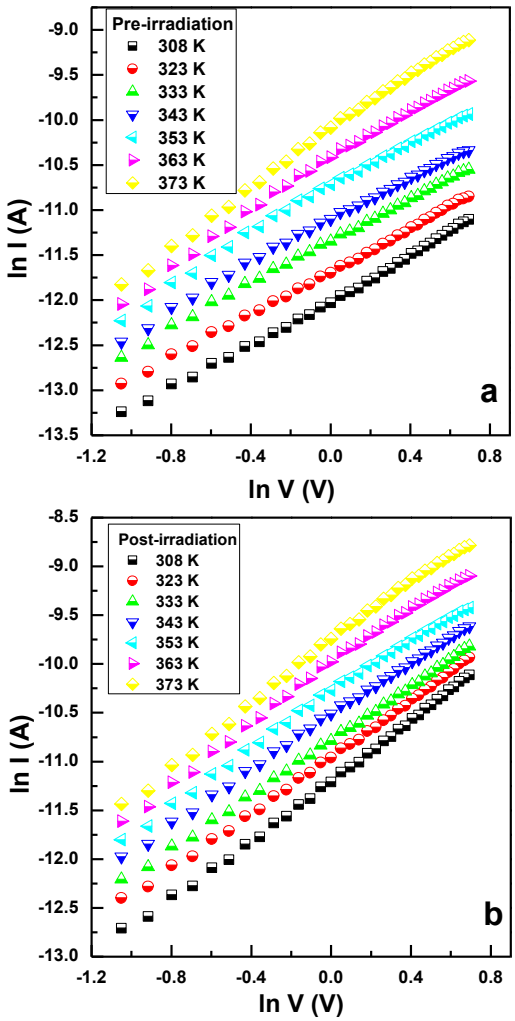

Figure 7 Variation of lnI versus lnV for (a) pre-irradiated Au/Bi_2Te_3/p-Si/Al diode and (b) post-irradiated Au/Bi_2Te_3/p-Si/Al diode measured at different temperatures.

According to Lambert theory, the current density in this region is given by [37]:

$$J = \frac{9}{8}\,\varepsilon\mu\theta\,\frac{V^2}{d^3}$$

Where d is the thickness of the Bi_2Te_3 film, ε is the permittivity of Bi_2Te_3, μ is the mobility of charge carrier and θ is the trapping factor, which is defined by the ratio of free charge to trapped charge and given by:

$$\theta = \frac{N_v}{N_t}\,exp\left(\frac{-E_t}{TK_B}\right)$$

Where N_v and N_t are the effective density of states in the valence band and the total trap concentration situated at energy level E_t above the valence band edge.

From the above expressions, according to that ln I versus the inverse of temperature should be a straight line as shown in **Figure 8.a and 8.b**. Using values of ε = 85 [38], μ= 680 $cm^2/V.s$ [39], and $N_v=2.265\times10^{24}$ cm^{-3} [40].

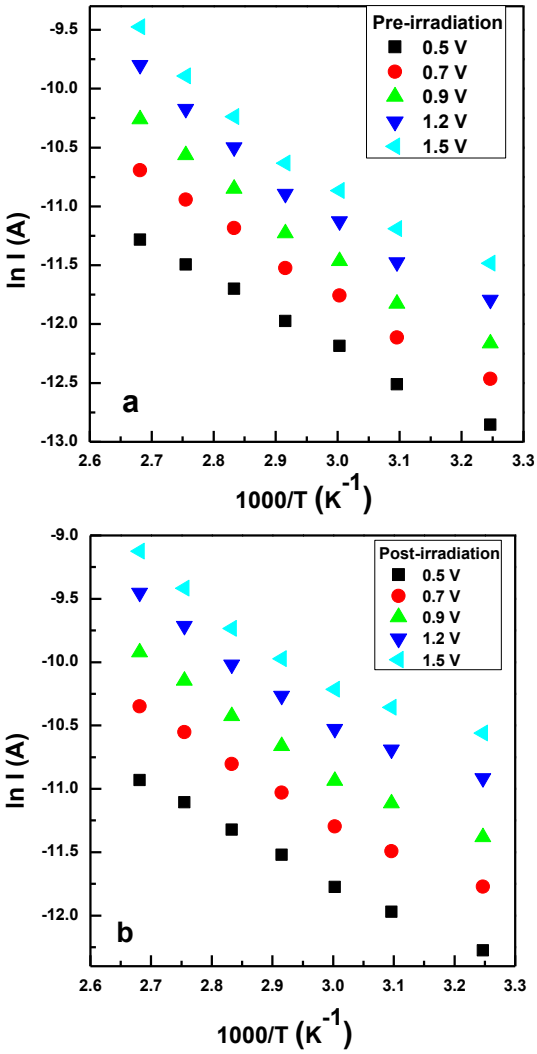

Figure 8 Temperature dependence of ln I in SCLC region for (a) pre-irradiated $Au/Bi_2Te_3/p$-Si/Al diode and (b) post-irradiated $Au/Bi_2Te_3/p$-Si/Al diode at different voltage.

The values of E_t and N_t for Au/n-Bi_2Te_3/p-Si/Al diode Schottky diode found to be 0.244 eV, 8.97×10^{45} cm^{-3} and 0.209 eV, 1.9×10^{46} cm^{-3} for pre-irradiation and post-irradiation respectively,

4. Summary and conclusions

The electrical properties of Unirradiated and irradiated Au/Bi_2Te_3/p-Si/Al diode was investigated. The barrier height, Φ_b, and ideality factor, n, for diodes were measured as a function of temperature. The estimated barrier height, Φ_b, was found to be increased as the annealing temperature was increased from 308 to 373k.

The ideality factor, n, of the fabricated device was increased with irradiation, but the ideality factor for device fabricated was decreased as annealing temperature was increased from 308 to 373 k. The investigated data showed that the X-ray irradiation has its impact on the thin films structure, where the particles are observed with higher aggregation, also has its impact on the electronic parameters of diodes, where Bi_2Te_3 diode showed decrease of its barrier height (ϕ_b) from 0.65 to 0.62 eV and increase of ideality factor from 2.67 to 3.03.

References.

[1] Giani A, Pascal Delannoy F, Boyer A, Foucaran A, Gschwind M,Ancey P. Elaboration of Bi2Te3 by metal organic chemical vapour deposition. Thin Solid Films; **303**:1–3 (1997)
[2] Mzerd A, Sayah D, Tedenac JC, Boyer A. Optimal crystal growth condition of thin films of Bi2Te3 semiconductors. J Cryst Growth; **140**:365–9 (1994)
[3] T. Lai, D. Alexiev, B.D. Nener, Journal of Applied Physics **78**: 3686 (1995)
[4] M. Edwards, G. Hall, S. Sotthibandhu, Nuclear Instruments and Methods **A310** : 283 (1991)
[5] S. Tataroglu, M.M.B ˘ ulb ¨ ul Altındal, Nuclear Instruments and Methods **A 568** : 863 (2006)
[6] V.A.J. Vanlint, Nuclear Instruments and Methods **A 253** : 453 (1987)
[7] G.E. Brehm, G.L. Pearson, Journal of Applied Physics **43** : 568 (1972)
[8] H.W. Kunert, D.J. Brink, Journal of Applied Physics **81** : 6948 (1997)
[9] C. Bjorkas, K. Nordlund, K. Arstila, J. Keinonen, V.D.S. Dhaka, M. Pessa, Journal of Applied Physics **100** : 053516 (2006)
[10] S. Chand, J. Kumar, Semicond. Sci. Technol. **11**: 1203 (1996)
[11] A. Singh, K.C. Reinhardt,W.A. Anderson, J. Appl. Phys. **68 (7)** 3478 (1990)
[12] A. Tataro˘glu, S , . Altındal, Nucl. Instrum. Methods **A 580** : 1588 (2007)
[13] P.G. McCafferty, A. Sellai, P. Dawson, H. Elabd, Solid-State Electron. **39**: 583 (1996)
[14] S. Chand, Semicond. Sci. Technol. **19** : 82 (2004)

[15] J.P. Sullivan, R.T. Tung, M.R. Pinto,W.R. Graham, J. Appl. Phys. **70**: 7403 (1991)
[16] W. Mondelaers, K. Van Laere, A. Goedefroot, K. Van den Bossche, Nucl. Instrum. Methods Phys. Res. **A368**: 278 (1996)
[17]H Koc, AM Mamedov, E Ozbay – Ferroelectrics, – Taylor &Francis, Optical Properties and Electronic Band Structure of Topological Insulators (on **A5 2B6 3** Compound Based) (2013)
[18] G. Wang and T. Cagin, Electronic structure of the thermoelectric materials Bi2Te3 and Sb2Te3from first-principles calculations. Phys Rev **B. 76**, 075201.1–075201.8 (2007).
[19]R. W. G. Wyckoff, Crystal Structures. New York: Wiley, **2** : 30 (1964)
[20]Bhakti Jariwala, Dimple shah, N.M. Ravindra, Influence of Doping on Structural and Optical Properties of Bi2Te3 Thin Films – Thin Solid Films **589** (2015)
[21]S. E. Harrison,1,a) L. J. Collins-McIntyre,2 S. Li,3 A. A. Baker,2,4 L. R. Shelford,4 Y. Huo,1A. Pushp,5 S. S. P. Parkin,5 J. S. Harris,1 E. Arenholz,6 G. van der Laan,4 and T. Hesjedal2,b , Study of Gd-doped Bi2Te3 thin films: Molecular beam epitaxy growth and magnetic properties - JOURNAL OF APPLIED PHYSICS **115**, 023904 (2014)
[22]M.M. El-Nahass, H.M. Zeyada, M.S. Aziz, M.M. Makhlouf, Thin Solid Films **492** : 290(2005)
[23]H.M. Zeyada et al. / Solar energy Materials & Solar Cells **92**: 1586-1592(2008)
[24] S.M. Sze, Physics of Semiconductor Devices, Wiley, New York, (1969)
[25] H.A.C. Etinkara, A. Turut, D.M. Zengın, S. Erel, Appl. Surf. Sci. **207**: 190 (2003)
[26] D.A. Neamen, Semiconductors Physics and Devices, R.R. Donnelley & Sons Company, Sydney, (1992)
[27] T.S.Shafai,T.D.Anthopoulos, Thin Solid Films **398** : 361 (2001)
[28]M.M. El-Nahass, Materials Chemistry and Physics **137** :716-722 (2013)
[29]C.-D. Lien, F. C. T. So, and M.-A. Nicolet, IEEE Trans. Electron Devices **31**, 1502 (1984).
[30]H.M. Zeyada, M.M. El-Nahass, E.M. El-Menyawy, A.S. El-Sawah, Electrical and photovoltaic characteristics of indium phthalocyanine chloride/p-Si solar cell. Synthetic Metals **207** : 46-53 (2015)
[31] S.N. Das, A.K. Pal, Semicond. Sci. Technol. **21**: 1557 (2006)
[32] I.S. Yahia, M. Fadel, G.B. Sakr, F. Yakuphanoglu, S.S. Shenouda, W.A. Farooq,J. Alloys Compd. **509** : 4414 (2011)
[33] F.A. Padovani, R. Stratton, Solid-State Electron **9** : 695 (1966)
[34] E.H. Rhoderick, IEE Proc. **129** (1982).
[35] L.S. Yu, Q.Z. Liu, Q.J. Xing, D.J. Qiao, S.S. Lau, J. Redwing, J.

Appl. Phys. **84** : 2099 (1998)
[36] S. Ashok, K.P. Pande, Solar Cells **14** : 61-81 (1985).
[37] M.A. Lampert, Rep. Prog. Phys. **27** : 329 (1964)
[38]Richter, W., Köhler, H., Becker, C. R.: Phys. Status Solidi (b) **84** : 619 (1977)
[39]CRC Handbook of Chemistry and Physics, David R. Lide, Ed. **79**th Edition, CRC Press, Boca Raton, FL, (1998)
[40]CRC Handbook of Chemistry and Physics, **93**rd Edition